Interplanetary Origins of Moderate (-100 nT < Dst ≤ -50 nT) Geomagnetic Storms During Solar Cycle 23 (1996-2008)

E. Echer[1], B. T. Tsurutani[2], W. D. Gonzalez[1]

[1] National Institute for Space Research (INPE), Av. dos Astronautas,1758, São José dos Campos, SP, 12227-010, Brazil.

eecher@dge.inpe.br, gonzalez@dge.inpe.br

[2] Jet Propulsion Laboratory, California Institute of Technology, 4800 Oak Grove Drive Pasadena, California 91109, Pasadena, CA, USA.

bruce.tsurutani@jpl.nasa.gov

Keywords: geomagnetic storms; solar wind; magnetosphere; solar cycle; space weather.

ABSTRACT

The interplanetary causes of 213 moderate intensity (-100 nT < peak *Dst* ≤ -50 nT) geomagnetic storms) that occurred in solar cycle 23 (1996-2008) are identified. Interplanetary drivers such as corotating interaction regions (CIRs), pure high speed streams (HSSs), interplanetary coronal mass ejections (ICMEs) of two types: those with magnetic clouds (MCs) and those without (non-magnetic cloud or ICME_nc), sheaths (compressed and/or draped sheath fields), as well as their combined occurrence, were identified as causes of the storms. The annual rate of occurrence of moderate storms had two peaks, one near solar maximum and the other in the descending phase, around 3 years later. The highest rate of moderate storm occurrence was found in the declining phase (25 storms.year^{-1}). The lowest occurrence rate was 5.7 storms.year^{-1} and occurred at solar minimum. All moderate intensity storms were associated with southward interplanetary magnetic fields, indicating that magnetic reconnection was the main mechanism for solar wind energy transfer to the magnetosphere. Most of these storms were associated with CIRs and pure HSSs (47.9%), followed by MCs and non-cloud ICMEs (20.6%), pure sheath fields (10.8%), and sheath and ICME combined occurrence (9.9%). In terms of solar cycle dependence, CIRs and HSSs are the dominant drivers in the declining phase and at solar minimum. CIRs and HSSs combined have about the same level of importance as ICMEs plus their sheaths in the rising and maximum solar cycle phases. Thus CIRs and HSSs are the main driver of moderate storms throughout a solar cycle, but with variable contributions from ICMEs, their shocks (sheaths), and combined occurrence within the solar cycle. This result is significantly different than that for intense (Dst ≤ -100 nT) and superintense (Dst ≤-250 nT) magnetic storms shown in previous studies. For superintense geomagnetic storms, 100% of the events were due to ICME events, while for intense storms, ICMEs, sheaths and their combination caused almost 80% of the storms. CIRs caused only 13% of the intense storms. The typical interplanetary electric field (E_y) criteria for moderate magnetic storms were identified. It was found that ~80.1% of the storms follow the criteria of $E_y \geq 2$ mV.m^{-1} for intervals longer than 2 hours. It is concluded that southward directed interplanetary magnetic fields within CIRs/HSSs may be the main energy source for long-term averaged geomagnetic activity at Earth.

1 Introduction

Geomagnetic storms are large-scale disturbances in the Earth's magnetosphere caused by enhanced solar wind-magnetosphere energy coupling and the growth of a storm-time ring current. Storms are usually defined by ground-based, low-latitude geomagnetic field horizontal component (H) variations (e.g., Gonzalez et al., 1994). The magnetic variations are proxies (and indirect measures) for disturbances in the plasma populations and current systems present in the magnetosphere (Dessler and Parker, 1959; Sckopke, 1966). It is well known that the primary interplanetary cause of geomagnetic storms is the presence of a southward interplanetary magnetic field (IMF) structures in the solar wind (Rostoker and Falthamahar, 1967; Hirsberg and Colburn, 1969; Akasofu, 1981; Gonzalez and Tsurutani, 1987; Tsurutani et al., 1988; Tsurutani and Gonzalez, 1997; Echer et al., 2005, 2008a). This magnetic field orientation allows magnetic reconnection (Dungey, 1961) to take place at the magnetopause and enhanced energy transfer from the solar wind to the Earth's magnetosphere.

The geomagnetic storm intensity is usually measured by the *Dst* index which is obtained from the disturbed geomagnetic field H-component measurements at low- and middle- latitude geomagnetic observatories (Sugiura, 1964; Rostoker, 1972). This index represents the magnetic depletion measured by low-latitude ground-based observatories due to an enhanced ring current formed by ions (mainly protons and oxygen ions) and electrons in the ~10-300 keV energy. The ring current is typically located between 2 and 7 R_E (Daglis and Thorne, 1999). Although the *Dst* index has contributions from other magnetospheric currents, the ring current energy content, both symmetric and asymmetric parts, has been considered to be well described by this index (Gonzalez et al., 1994).

Intense geomagnetic storms (peak $Dst \leq$ -100 nT) and their interplanetary origins have been widely studied (Tsurutani et al., 1988; 1992; 1995; 2006a, b; Gonzalez et al., 1999, 2007, 2011; Gonzalez and Echer, 2005; Zhang et al., 2006; 2007; Echer et al., 2008a).

In comparison, only a few studies have been performed on moderate (-50 nT ≤ *Dst* <-100 nT) storms (Tsurutani and Gonzalez, 1997; Wang et al., 2003; Zhang et al., 2006; Xu et al., 2009; Echer et al., 2011; Hutchinson et al., 2011;Tsurutani et al., 2011). None of the previous studies were done over an entire solar cycle. It is the purpose of this paper to perform a statistical study the interplanetary origins and conditions leading to moderate storms during solar cycle 23 (SC23) from 1996 to 2008. This study is intended to complement the intense (*Dst* ≤ -100 nT) and superintense (*Dst* ≤ -250 nT) storm studies previously done on SC23 (Gonzalez et al., 2007; Zhang et al., 2007; Echer et al., 2008a, b). We will discuss the differences of the interplanetary drivers for moderate storms compared to those of intense and superintense events.

2 Methodology of data analysis

A list of geomagnetic storms with peak *Dst* ≤ -50 nT was compiled by Echer et al. (2011). From this list, the subset of moderate geomagnetic storms (-100 nT < *Dst* ≤ -50 nT) during SC23 (1996-2008) was identified. This period for solar cycle 23 was defined using the smoothed sunspot number criterion of solar cycle minimum and maximum (e.g, Hathaway, 2010). During this interval, 213 moderate geomagnetic storms were identified and are used in this study.

The NASA GSFC OMNIWEB (http://omniweb.gsfc.nasa.gov/ow.html) solar wind parameters were used to obtain solar wind peak speed (V_{sw}), southward directed IMF component (B_s) and the dawn-to-dusk directed component of the interplanetary convection electric field (E_y) values. Sunspot numbers were obtained from the Solar Influences Data Analysis Center, (http://www.sidc.be). Geomagnetic Dst indices were obtained from the World Data Center for Geomagnetism – WDC Kyoto (swdcwww.kugi.kyoto-u.ac.jp/).

The high resolution (~1-minute) solar wind data were analyzed and the interplanetary structures identified using the criteria mentioned in Echer et al. (2006, 2008a). For the identification of the interplanetary causes we have followed the nomenclature and definitions given by Burlaga et al. (1981), Tsurutani et al. (1988, 1995, 2006a, b), Balogh et al. (1999), Gonzalez et al. (1999, 2007), and Echer et al. (2008a). They are: corotating interaction regions (CIRs), interplanetary coronal mass ejections (ICMEs) of the type magnetic cloud (MC) and non-magnetic cloud (ICME_nc), interplanetary shocks/sheaths, i.e, fields in the sheath or shocked/compressed fields (SHOCK), pure high speed streams following CIRs (HSS), and combinations of the above structures. By —ICME of the MC type we mean those cases with clear field rotations. There were other types of solar wind disturbances that could not be easily identified and these are identified as (DISTURB_SW). On rare occasions, no solar wind data was available (DATA GAP).

The identification of structures was checked by examining the list of ICMEs at http://www.srl.caltech.edu/ACE/ASC/DATA/level3/icmetable2.htm (Richardson and Cane, 2010), the list of high speed streams (HSSs) at http://www.spacescience.ro/new1/HSS_Catalogue.html (Maris and Maris, 2003), the ACE spacecraft list of interplanetary shocks (http://espg.sr.unh.edu/mag/ace/ACElists/obs_list.html#shocks), the ICME list at http://www-ssc.igpp.ucla.edu/~jlan/ACE/Level3/ICME_List_from_Lan_Jian.pdf (Jian et al., 2006).

In all cases our own judgment was used in the final decision of the interplanetary structure classifications. Fast forward shocks were identified by simultaneous sharp increases in the solar wind speed, density, temperature and magnetic field where the derived shock speed (from the Rankine-Hugoniot relations) was greater than the upstream magnetosonic speed (Tsurutani et al., 2011). ICMEs were identified by high magnetic field magnitude low beta regions sunward of the interplanetary shocks and sheaths (Tsurutani et al., 1997). If the ICME contained significant By or Bz rotations, it was identified as a MC. If not, it was labeled as an ICME_nc event (Burlaga et al., 1982; Echer et al., 2008). High speed streams had speeds up to 750 to 800 km/s, but not higher. A coronal hole near the subsolar point was identified as the origin of each high speed stream. The compressed magnetic field intensity (and plasma density) at the antisunward edge of the high speed streams were identified as CIRs (Balogh et al., 1999; Tsurutani et al., 2011b). The disagreement between our assessments and other authors was about 5% of the storms (about 10 of 213 storms).

Out of the 213 moderate magnetic storms, 211 had sufficiently complete interplanetary data to be able to identify the interplanetary drivers. Out of the 211 events, 199 of them fit into one of the many categories (all associated with either ICMES or CIRs/HSSs).

In this paper we examine interplanetary structures and solar wind parameters (peak V_{sw}, peak B_z, and peak E_y) during the storm main phase. Thus we did not consider interplanetary structures and parameters that follow the peak *Dst*, features that were associated with the storm recovery phase.

3 Results and Discussion

3.1 Examples of moderate geomagnetic storms

Figure 1 shows a moderate geomagnetic storm caused by a MC on 16-17 April, 1999. Panels are the ACE spacecraft 64-s averaged solar wind speed (V_{sw}), proton density (N_p), proton temperature (T_p), IMF components B_x, B_y, and B_z in GSM coordinates, IMF magnitude (B_o) and the 1-hour *Dst* index. The shock and MC boundaries are marked with dotted and dashed vertical lines. The storm main phase is indicated by a vertical arrow and with **—***mp"* in the *Dst* panel. An interplanetary shock is observed at ~1130 UT on April 16. The MC began at ~1800 UT on 16 April and lasted until ~1900 UT on 17 April. The MC was a south-north structure (SN). The first part of the magnetic cloud, with negative B_z, was responsible for the magnetic storm with a peak *Dst* of -91 nT at ~0800 UT on April 17 1999. Peak interplanetary parameters for this storm were V_{sw} = 430 km/s, B_s = 14.0 nT, and E_y = 6.0 mV.m^{-1}.

Figure 2 shows a moderate geomagnetic storm caused by a CIR from 21 to 23 May 2003. The storm main phase started at ~1400 UT on 21 May 2003 and ended at ~0300 UT on 22 May 2003. A peak *Dst* value of -73 nT is reached this time. The Figure 2 panels have the same format as those in Figure 1. The CIR can be identified by the simultaneous magnetic field magnitude and plasma density increases. There is neither a forward shock at the leading edge nor a reverse shock at the trailing edge. The CIR is located between the slow speed stream (SSS) and the high speed stream (HSS). The southward IMF magnetic fields within the CIR were responsible for the moderate magnetic storm. Peak interplanetary parameters for this storm were V_{sw} =522 km/s, B_s = 6.7 nT, and E_y = 3.5 mV.m^{-1}.

Figure 3 shows a moderate geomagnetic storm caused by sheath fields following a shock (SHOCK/SHEATH) on 13 September 2001. The panel format is the same as in

Figure 1. The storm main phase lasted from ~0200 UT on 12-13 September 2001 to ~0800 UT on 13 September 2001. A peak *Dst* value of -57 nT is reached this time. The storm main phase is identified by a vertical arrow. The shock can be identified by a dotted line as the abrupt jump in solar wind parameters. The density and magnetic field downstream to upstream ratios are ~1.5. Southward IMFs within the sheath fields were responsible for the magnetic storm. Peak interplanetary parameters for this storm were V_{sw} = 405 km/s, B_s = 9.7 nT, and E_y = 3.8 mV.m^{-1}.

Figure 4 shows a moderate geomagnetic storm caused by a pure HSS on 07-08 March 2005. The panels in Figure 4 have the same format as those in Figure 1. The storm main phase lasted from ~1800 UT on 07 March to ~0800 UT on 08 March 2005. The storm had a peak *Dst* value of -59 nT. This interval corresponded to a pure coronal hole HSS, which followed a CIR. The cause of this storm was the presence of southward components of Alfvénic fields in the HSS. Peak interplanetary parameters for this storm were V_{sw} ~ 750 km/s, B_s = 3.8 nT, and E_y = 2.8 mV.m^{-1}.

Figure 5 shows a moderate geomagnetic storm caused by a combination of MC and CIR/HSS on 03-06 April 2004. The storm main phase lasted from ~0300 UT to ~1000 UT on 06 April 2004. The storm had a peak *Dst* value of -81 nT. Southward components of the IMF were correlated with the storm main phase. The MC lasted from ~0000 UT on 04 April to ~1800 UT on 05 April 2004. The CIR and HSS were detected immediately following the MC. Peak interplanetary parameters for this storm were V_{sw} = 419 km/s, B_s = 15.7 nT, and E_y = 6.3 mV.m^{-1}.

The above are some typical cases studied in this survey. For all cases where there were interplanetary data, it was found that southward IMFs were present during the main phase of the magnetic storm. Thus it appears that magnetic reconnection between the solar wind IMF and the magnetosphere is the main mechanism that is responsible for energy transfer to the magnetosphere during moderate storms. The focus of this study is —what are the interplanetary structures responsible for these southward IMFs? We will address this in the statistical part of the study.

3.2 Statistics of moderate geomagnetic storms

3.2.1 – General statistics analysis

Figure 6 shows the number of moderate storms per year (bars) and the annual sunspot number average (solid line). It can be seen that the moderate storm occurrence rate has two peaks in the solar cycle. One peak is near solar maximum (2001) and other in the descending phase (in 2003 and 2005). This latter peak is centered ~3 years after the first.

Figure 7 shows the correlation between peak *Dst* and peak V_{sw} (top panel), peak *Dst* and peak B_s (intermediate panel), and peak *Dst* and peak E_y (bottom panel). The correlation of *Dst* with solar wind parameters was modest. The *Dst* correlation with E_y had a *r* value of 0.55 and that with B_s had a *r* value of 0.48. The correlation between *Dst* and Vsw is very low (r = 0.08), essentially negligible.

The average peak values of solar wind during all moderate storms where there were interplanetary data were V_{sw} = 517 ± 120 km/s, B_s = 8.4 ± 3.1 nT and E_y = 4.0 ± 1.4 mV.m^{-1}, respectively. The interplanetary E_y criteria were studied and it was found that 173 storms (81.2%) followed the criteria of E_y > 2 mV.m^{-1} for 2 hours, 102 storms (47.9%) of E_y > 3 mV.m^{-1} for 2 hours, and 40 storms (18.8%) of E_y >4 mV.m^{-1} for 2 hours.

The association of interplanetary structures causing the main phase of moderate storms is shown in Table 1. The nomenclature follows the one presented in the Methodology Section.

Most of the storms were associated with CIRs (32.4%). Non-cloud ICMEs were the second most frequently occurring phenomenon (14.5%). Sheath fields (10.8%) and pure

HSSs (10.8%) were the third most frequent. MCs were responsible for 6.1% of the moderate storms. Combinations of shock-ICME fields and shock-MC fields accounted for 5.2% and 4.7% of the cases, respectively.

The above categories can be clustered into: coronal hole corotating streams (CIR + HSS and their combination), CME transients (ICME_nc and MC), shock/sheath fields, and the combination of shock/sheath fields, ICME_nc, and MC. In Figure 8, a sector graph is shown giving the percentage of moderate geomagnetic storms caused by different interplanetary structures. It can be noted that 47.9% of the storms are associated with CIRs and pure HSSs following CIRs and their combination. Thus HSSs and CIRs are the most probably cause of moderate magnetic storms over the solar cycle. MCs or non-cloud ICMEs accounted for 20.6% of moderate magnetic storms. Furthermore, 10.8% of the storms were associated with shock/sheath fields, and 9.9% of the storms with combinations of non-cloud ICME or MC with sheath fields. About 10.8% of the moderate storms were not caused by any of the above categories.

3.2.2 - Solar Cycle Phase Dependence of Interplanetary Drivers

The occurrence frequency of the various types of interplanetary causes of moderate storms throughout solar cycle 23 was studied. The solar cycle was divided into: the solar cycle rising phase (1997-1999, 53 storms), the maximum phase (2000-2002, 62 storms), the declining phase (2003-2005, 75 storms) and lastly the minimum phase (1996 and 2006-2008, 23 storms). Table 2 shows the major interplanetary structures causing moderate storms during the different phases of solar cycle 23. It can be noted that CIRs and HSSs are the overwhelming cause of moderate storms at solar minimum (82.6% of the storms). They are responsible for almost ~2/3 of the storms in the declining phase (60.0%), and also are the leading causative interplanetary structure in the rising and solar maximum phases (30-34%). ICMEs (both MC and ICME_nc) are the second major cause, with higher relative importance in the rising phase and at solar maximum. Shock/sheath fields and combination of sheath and ICME fields came next. The preceding category had relatively higher importance in the solar cycle rising and maximum phases.

From the Table 2 one can calculate the moderate storm occurrence rate as a function of the phase of the solar cycle. In the rising phase there were 17.7 storms.year^{-1}, and in the solar maximum phase there were 20.7 storms.year^{-1}. The solar cycle declining phase had the highest frequency of moderate magnetic storms (25 storms.year^{-1}), and solar minimum phase had the minimum in frequency of magnetic storms (5.7 storms.year^{-1}).

4 Summary and Discussion

4.1 Comparison to previous moderate storms (Dst ≤ -50 nT) surveys

Tsurutani and Gonzalez (1997) studied the interplanetary association of moderate storms during an ISEE-3 1978-1979 solar maximum interval. They found that ~40% of storms were associated with shocks/ICMEs, ~23% to high-speed streams 14 without shocks, ~17% to high-low speed stream interactions (CIRs), ~10% to noncompressive density enhancements and ~10% related to other phenomena, including Alfvénic fluctuations. If we compare our present results for only the solar maximum portion of SC 23, we find that ~33.9% of the storms were associated with CIRs and HSSs, 22.6% with non-cloud and MC ICMEs, 16.1% with pure shock/sheath fields and 14.5% with combination of shock/sheath and ICME fields. If the last 3 categories are combined, it is found that shock/sheath MC and ICME non MC account for 43% of the moderate magnetic storms during the SC 23 maximum. This is in good accord with the Tsurutani and Gonzalez (1997) result for SC 21. If we combine their results for HSSs and high speed stream-low speed stream interactions, they have 40-50% of moderate storms associated with HSSs and their effects. Again our results are in good agreement with the SC21 solar maximum study.

Xu et al. (2009) have studied geomagnetic storms during part of solar cycle 23 (1998-2008). They found that 40% of moderate storms were associated to CIRs, 31% to MCs, 15% to non-cloud ICMEs (these last categories including shock contribution), 5% to shocks/sheaths, and 9% to other phenomena. These percentages differ slightly with the results obtained in this paper: CIRs and pure HSSs caused 47.9% of the moderate storms, followed by ICMEs of MC and non-cloud types at 20.6%, shock fields at 10.8%, and shock and ICME combined occurrence at 9.9%. However we note that in the present work two additional years were included (1996-1997) in order to fill out SC23. In these two years there was a large contribution of moderate storms caused by CIRs. Thus our percentage of storms caused by CIRs is higher in this work than in the Xu et al (2009). There is also a difference in the percentage of storms that were caused by ICMEs and ICMEs combined with shock/sheaths (~40% in this work and ~46% in Xu et al. 2009), caused partially by the two additional years and also perhaps by different methodologies. The highest number of moderate storms was observed by Xu et al. (2009) in 2003. In this paper the highest peak was observed in 2003, but with another important (secondary) peak close to solar maximum.

4.2 Comparison to results for intense (Dst ≤-100 nT) storms and superintense (Dst <- 250 nT) storms

The interplanetary drivers for intense and superintense storms are substantially different than for moderate storms. For intense (-100 nT ≤ *Dst* ≤ -250 nT) storms, magnetic clouds, shock/sheath fields, and sheath fields are the primary causes. CIRs and HSSs are secondary in importance (Gonzalez et al., 2007, Echer et al., 2008a). For superintense storms (*Dst* < -250 nT) the interplanetary causes were MCs, shocks/sheaths and combination of shocks/sheaths and MCs (Tsurutani et al., 1992; Echer et al., 2008b). CIRs and HSSs did not cause any of the superintense magnetic storms. Thus the role of CIRs in causing storm main phases decreases with increasing storm strength.

The correlation of peak *Dst* with solar wind parameters (B_s, E_y) during moderate storms was lower than for intense storms (Echer et al., 2008a). The correlation of *Dst* with E_y was $r = 0.55$, and for *Dst* with B_s, $r = 0.48$. The correlation between *Dst* and V_{sw} was very low $r = 0.08$. For intense storms during SC23 it was found that the *Dst*-B_s correlation had a $r = 0.80$. For *Dst*-E_y, $r = 0.84$. For *Dst*-V_{sw}, $r = 0.55$ (Echer et al., 2008a). It is possible that

Alfvénic fluctuations and other solar wind features have reduced the correlations for moderate storms because Dst often does not have a steady, clear average or minimum.

It was found that 80.1% of the moderate storms follow the criteria of $E_y \geq 2$ mV.m^{-1} for an interval longer than 2 hours. This can be contrasted with the intense storm criteria of $E_y \geq 5$ mV.m^{-1} for 3 hours (Gonzalez and Tsurutani, 1987). Echer et al. (2008a) found that 70% of storms follow the Ey > 5mV.m^{-1} for 3 hr criteria, and 90% following the criteria of $E_y \geq 3$ mV.m^{-1} for at least 3 hours. The present result agrees reasonably well with the threshold for moderate storms of $E_y \geq 2.5$ mV.m^{-1} for duration longer than 2 hours derived by Gonzalez et al.(1994). 336

The rates of moderate storms in the present study (Table 3) were found to be 20.7 storms.year^{-1} in the solar maximum phase, 25 storms.year^{-1} in the solar cycle declining phase, and 5.7 storms.year^{-1} in the minimum phase. Echer et al. (2008a) found an intense storm rate of 8.5 storms.year^{-1} at solar maximum and 3-6.5 storms.year^{-1} in the other solar cycle phases. Thus our moderate storm rate is higher than the intense storm rate by a factor of ~4 at solar maximum and ~5 times higher during the declining phase. At solar minimum the moderate storm and intense storm occurrence rates are about comparable.

The average solar wind (peak) parameters during moderate storms were $V_{sw} = 517$ km/s, $B_s = 8.4$ nT and $E_y = 4$ mV.m^{-1}. This can be compared with solar wind parameters during intense and superintense storms. For intense storms, average values are $V_{sw} = 605$ km/s, B_s =18.3 nT *and* $E_y = 10.7$ mV.m^{-1} (Echer et al., 2008). For superintense storms average values are $V_{sw} =$ 799.1 km/s, $B_s = 34.3$ nT *and* $E_y = 23.5$ mV.m^{-1} (Gonzalez et al., 2011). Note that the average value of B_s and E_y almost doubles going from moderate storms to intense storms. It again doubles going from intense storms to superstorms. One can conclude that the energy input into the magnetosphere for the above classes of magnetic storms has an increment of at least a factor of ~2.0. Other solar wind parameters (speed, density, field orientation) must be taken into account to calculate the accurate energy input.

5 Conclusions

In this work, a detailed study of interplanetary conditions causing moderate storms during a full solar cycle was performed. It was found that moderate storms have two occurrence rate peaks in solar cycle 23, similar to that of intense storms. The latter has reported for previous solar cycles (Gonzalez et al., 1990; Echer et al., 2011). The correlation with the interplanetary/solar wind parameters was much lower than for intense storms. Also, moderate storms were associated with E_y, but with lower E_y values and shorter durations than for intense storms. The latter relationship was expected.

Figure 9 shows the distribution of the percentage of storms caused by CIRs and HSSs as function of solar cycle phase. For comparative purposes, the distributions for intense and superintense storms are also shown. The blue, green and red bars show the occurrence of moderate (-100 nT < $Dst \leq$ -50 nT), intense (-250 nT < $Dst \leq$ -100 nT) and superintense storms ($Dst \leq$ -250 nT) caused by CIRs. The moderate storm statistics are taken from this study. The intense storm statistics come from Gonzalez et al. (2007) and Echer et al. (2008a). The superintense storms are taken from Tsurutani et al. (1992) and Echer et al. (2008b). The percentage of storms caused by other interplanetary structures is also shown. It can be noted that no superstorms were caused by CIRs. Both moderate and intense storms have a larger contribution from CIRs during the solar minimum and declining phases, and lower during the solar maximum and rising phases. CIRs can cause up to ~60% and ~80% of moderate storms, during the declining and minimum phases, respectively, and up to ~20% and 30% of intense storms in the same phases.

The major interplanetary causes of moderate storms are CIRs/HSSs, followed by ICMEs. This contrasts with superintense ($Dst \leq$-250 nT) storms, for which the major causes are ICMEs, sheath fields and their combination.

It can be concluded that CIRs and their associated HSSs are the major driver of moderate geomagnetic storms throughout a solar cycle, but with variable contribution of ICMEs (non-clouds and MCs) and shocks/sheaths.

Final Comments

Previous studies that have focused on the geoeffectiveness of CIRs and high speed streams have indicated that taken over several day intervals, CIRs/high speed streams are more geoeffective, i.e., they are more important than ICMEs for driving long-term average geomagnetic activity (Tsurutani et al., 1995; 2006a, b; Alves et al., 2006; 2011; Echer et al., 2006; Kozyra et al., 2006; Guarnieri, 2006; Turner et al., 2006). These studies arrived at their conclusions based on calculations of energy input into the magnetosphere using *Dst* and *AE* proxies. This present result indicates that the dominant solar wind drivers for moderate magnetic storms for SC 23 are CIR/HSSs drivers. Thus when considering all levels of solar wind energy transfer to the magnetosphere, it is clear that CIR/HSSs is the major factor for energy transfer to the Earth's magnetosphere over time spans of solar cycles (~10 to 14 years).

Acknowledgements

The authors would like to acknowledge the NASA Goddard Space Flight Center through the *Space Physics Data Facility* (OMNIWEB solar wind data base), the Solar Influences Data Analysis Center, and the World Data Center for Geomagnetism-Kyoto, for providing solar wind, sunspot and geomagnetic Dst data. One of the authors (EE) would like to thanks to the Brazilian CNPq (301233/2011-0) agency or financial support. Portion of this research was done at the Jet Propulsion Laboratory, California Institute of Technology under contract with NASA.

References

Akasofu, S. I., Energy coupling between solar wind and magnetosphere, Space Sci. Rev., 1981.

Alves, M. V., Echer, E., Gonzalez, W. D., Geoeffectiveness of corotating interaction regions as measured by Dst index, J. Geophys. Res., 111, A07S05, 2006.

Alves, M. V., Echer, E., Gonzalez, W. D., Geoeffectiveness of solar wind interplanetary magnetic structures, J. Atmos. Solar-Terr. Phys., 73, 1380-1384, 2011.

Balogh A, Bothmer V, Crooker NU, Forsyth RJ, Gloeckler G, Hewish A, Hilchenbach M, Kallenbach R, Klecker B, Linker JA, Lucek E, Mann G, Marsch E, Posner A, Richardson IG, Schmidt JM, Scholer M, Wang YM, Wimmer-Schweingruber RF, Aellig MR, Bochsler P, Hefti S, Mikic Z, Corotating interaction regions, Space Sci. Rev., 89, 141, 1999.

Burlaga, L. F., Sittler, E., Mariani, F., Schwenn, R., Magnetic loop behind an interplanetary shock: Voyager, Helios and IMP-8 observations, J. Geophys. Res., 86(A8), 6673– 6684, 1982.

Daglis, I. A. and Thorne, R. M., The terrestrial ring current: origin, formation, and decay, Reviews of Geophysics, 37,407-438, 1999.

Dessler, A. J., Parker, E., Hydromagnetic theory of magnetic storms, J. Geophys. Res., 64, 2239-2259, 1959.

Dungey, J. W., Interplanetary magnetic field and the auroral zones. Phys. Rev. Lett. 6, 47–48, 1961.

Echer, E., Gonzalez, W. D., Guarnieri, F. L., Dal Lago, A. , and Vieira, L. E. A., Introduction to space weather, Advances in Space Research, 35, 855-865, 2005.

Echer, E., Gonzalez, W. D., Alves, M. V., On the geomagnetic effects of solar wind interplanetary magnetic structures, Space Weather, 4, S06001, doi:10.1029/2005SW000200, 2006.

Echer, E., Gonzalez, W. D., Tsurutani, B. T., Gonzalez, A. L. C., Interplanetary conditions causing intense geomagnetic storms (Dst ≤ -100 nT) during solar cycle 23 (1996-2006), J. Geophys. Res., 113, A05221, doi:10.1029/2007JA012744, 2008a.

Echer, Gonzalez, W. D., Tsurutani, B. T., Interplanetary conditions leading to superintense geomagnetic storms (Dst < -250) during solar cycle 23, Geophys. Res. Lett., 35, L06S03, doi:10.1029/2007GL031755, 2008b.

Echer, E., Gonzalez, W. D., Tsurutani, B. T., Statistical studies of geomagnetic storms with peak Dst ≤ -50 nT from 1957 to 2008, J. Atmos. Solar-Terr. Phys., 73, 1454-1459, 2011.

Gonzalez, W.D., Tsurutani, B. T., Criteria of interplanetary parameters causing intense magnetic storms (Dst < -100 nT), Planet. Space Sci., 35,1101, 1987.

Gonzalez, W. D., Gonzalez, A. L. C., Tsurutani, B. T., 1990. Dual-peak solar cycle distribution of intense geomagnetic storms, Planet. Space Sci., 38, 181-187, 1990.

Gonzalez, W. D.¸ Joselyn, J. A., Kamide, Y., Kroehl, H. W., Rostoker, G., Tsurutani, B. T., Vasyliunas, V., What is a geomagnetic storm Journal of Geophysical Research, 99, 5771-5792, 1994.

Gonzalez, W.D., Tsurutani, B.T., Clua de Gonzalez, A. L., Interplanetary origin of geomagnetic storms. Space Sci. Rev. 88, 529–562, 1999.

Gonzalez, W. D., Echer, E., A study on the peak Dst and peak negative Bz relationship during intense geomagnetic storms, Geophys. Res. Lett., 32, L18103, doi:10.1029/2005GL023486, 2005.

Gonzalez W. D., Echer, E., Clua-Gonzalez, A. L., Tsurutani, B. T., Interplanetary origin of intense geomagnetic storms (Dst < −100 nT) during solar cycle 23, Geophys. Res. Lett., 34, L06101, doi:10.1029/2006GL028879, 2007.

Gonzalez, W. D., Echer, E., Tsurutani, B. T., Clua de Gonzalez, A. L., Dal Lago, A., Space Science Reviews, 158, 69-89, 2011.

Hathaway, D. H., (2010), The solar cycle, Living Rev. Solar Phys., 7, 1., 2010.

Hirshberg, J., Colburn, D. S., Interplanetary field and geomagnetic variations, aunified view, Planet. Space Sci., 17, 1183-1206, 1969.

Hutchinson, J. A., Wright, D. M., Milan, S. E., Geomagnetic storms over the last solar cycle: A superposed epoch analysis, J. Geophys. Res., 116, A09211, 2011.

Jian L. C. T. Russell, J. G. Luhmann and R. M. Skoug, Properties of Interplanetary Coronal Mass Ejections at One AU During 1995 – 2004Solar Physics 239, 393, 2006.

Maris, O., and Maris, G., High-speed plasma streams in solar wind, Romanian Reports in Physics, 55, 3, 259-269, 2003.

Richardson, I., Cane, H. V., Near-Earth interplanetary coronal mass ejections during solar cycle 23 (1996-2009): Catalog and summary of properties, Solar Physics, 2010.

Rostoker, G., Falthammar, C. G., Relatinoship between changes in the interplanetary magnetic field and variations in the magnetic field at Earth's surface, J. Geophys. Res. 72, 5853, 1967.

Rostoker, G. Geomagnetic indices, Review of Geophysics, 10, 935—950, 1972.

Sckopke, N., A general relation between energy of trapped particles and disturbance field near earth, J. Geophys. Res., 71, 3125, 1966.

Sugiura, M., Hourly values of equatorial Dst for the IGY, Annual International Geophysical Year, vol. 35, p. 9, Pergamon, New York, 1964.

Tsurutani, B.T., Gonzalez, W. D., Tang, F., Akasofu, S. I., Smith, E. J., Origin of interplanetary southward magnetic fields responsible for major magnetic storms near solar maximum (1978-1979), J. Geophys. Res., 93, 8519, 1988.

Tsurutani, B. T., W. D. Gonzalez, F. Tang, and Y. T. Lee , Great magnetic storms, Geophys. Res. Lett., 19, 73., 1992.

Tsurutani, B. T., Gonzalez, W. D., Gonzalez, A. L. C., Tang, F., Arballo, J., Okada, M., Interplanetary origin of geomagnetic activity in the declining phase of the solar cycle, J. Geophys. Res., 100(A11), 21,717– 21,733, 1995.

Tsurutani, B. T., Gonzalez, W. D, The interplanetary causes of magnetic storms; a review, in (Eds) B Tsurutani, W. D. Gonzalez, Y. Kamide, J. K. Arballo, Magnetic storms, AGU Geophysical Monograph 98, 77-89, 1997.

Tsurutani, B. T.,Gonzalez, W. D., Gonzalez, A. L. C., Guarnieri, F. L., Gopalswamy, N., Grande, M., Kamide, Y., Kasahara, Y., Lu, G., Mann, I., McPherron, R., Soraas, F., Vasyliunas, V., Corotating solar wind streams and recurrent geomagnetic activity, a review, J. Geophys. REs., 111, A07S01, 2006a.

Tsurutani, B. T., McPherron, R. L., Gonzalez, W. D., Lu, G., Gopalswamy, N., Guarnieri, F. L. Magnetic storms caused by corotating solar wind streams, AGU Monograph 167, Recurrent magnetic storms, corotating solar wind streams,2006b.

Tsurutani, B. T., Echer, E., Guarnieri, F. L., Gonzalez, W. D., The properties of two solar wind high speed streams and related geomagnetic activity during the declining phase of solar cycle 23, J. Atmos. Solar-Terr. Phys., 73, 164-177, 2011a.

Tsurutani, B. T., Lakhina, G. S., Verkhoglyadova, O. P., Gonzalez, W. D., Echer, E., Guarnieri, F. L., A review of interplanetary discontinuities and their geomagnetic effects, J. Atmos. Solar-Terr. Physics, 73, 5-19, 2011b.

Xu, D., Chen, T., Zhang, X. X., Liu, Z., Statistical relationship between solar wind conditions and geomagnetic storms in 1998-2008, Planetary and Space Science, 57, 1500-1513, 2009.

Wang, Y., Shen, C. L., Wang, S., Ye, P. Z., An empirical formula relating the geomagnetic storm’s intensity to the interplanetary parameters, Geophys. Res. Lett., 30, 20, 2039, 2003.

Zhang, J., Liemonh, M. W., Kozyra, J. U., Thomsen, M. F., Elliott, H. A., Weygand, J. M., A statistical comparion of solar wind sources of moderate and intense geomagnetic storms at solar minimum and maximum, J. Geophys. Res., 111, A01104, 2006.

Zhang, J., Richardson, I. G., Webb, D. F., Gopalswamy, N., Huttunen, E., Kasper, J. C., Nitta, N. V., Poomvises, W., Thompson, B. J., Wu, C.-C., Yashiro, S., Zhukov, A. N.. Solar and interplanetary sources of major geomagnetic storms (Dst< 100 nT) during 1996– 2005, J. Geophys. Res., 112, A10102, doi:10.1029/2007JA012321, 2007.

Figure captions

Figure 1 – Moderate geomagnetic storm caused by a MC in 16-17 April, 1999. Panels are ACE 64-s averaged solar wind speed (V_{sw}), proton density (N_p), proton temperature (T_p), IMF components in GSM (B_x, B_y, B_z), IMF magnitude (B_o) and *Dst* index. The shock is marked with dotted lines, and the MC with an arrow. The storm main phase is marked with a vertical arrow and with *mp* in the *Dst* panel (The same for Figures 2 to 5).

Figure 2 – Moderate geomagnetic storm caused by a CIR in 20-23 May 2003. Panels are the same as in Figure 1. The interaction region, the low and high speed solar wind intervals are marked with labels (CIR, LSS and HSS).

Figure 3 – Moderate geomagnetic storm caused by sheath fields (shock marked as S) in 13 September 2001. Panels are the same as in Figure 1.

Figure 4 – Moderate geomagnetic storm caused by a pure HSS in 07-08 March 2005. Panels are the same as in Figure 1. The HSS is marked in the top panel.

Figure 5 – Moderate geomagnetic storm caused by a MC and CIR/HSS in 05-06 April 2004. Panels are the same as in Figure 1. The MC, CIR and HSS are marked in the top panel.

Figure 6 – Number of moderate storms (Dst ≤ -50 nT) pear year (bars) during 1996- 2008 and annual sunspot number average (solid line).

Figure 7 – Correlation between peak *Dst* (-*Dst*) and peak V_{sw} (top panel), peak *Dst* and peak B_s (intermediate panel), and peak *Dst* and peak E_y (bottom panel) for moderate storms during solar cycle 23. The linear fit is shown as dashed line and the correlation coefficients are shown in the top left corner.

Figure 8– Sector graph showing the percentage of moderate geomagnetic storms in solar cycle 23 caused by major interplanetary structures.

Figure 9 – Solar cycle (phases) distribution of the percentage of moderate, intense and superintense geomagnetic storms caused by CIRs-HSSs.

Table captions

Table 1 – Association of the 213 moderate geomagnetic storms in solar cycle 23 with interplanetary structures with B_s fields that caused the storm main phases.

Table 2 – Major interplanetary structures causing moderate storms along the different phases of solar cycle 23.

Table 1

IP Structure	Acronym	Number of storms (percentage)
Corotating interaction region between fast and slow solar wind streams	CIR	69 (32.4%)
Interplanetary coronal mass ejection that does not have the MC signature	ICME_nc	31 (14.5%)
Shocked fields, intensified by compression or draping effects	SHOCK/SHEATH	23 (10.8%)
Pure high speed stream	HSS	23 (10.8%)
Interplanetary coronal mass ejection of the MC type	MC	13 (6.1%)
Solar wind disturbance not identified in the classes above	DIST_SW	12 (5.6%)
Combination of shock, sheath and non-MC ICME fields	SHOCK-ICME_nc	11 (5.2%)
Combination of shock, sheath and MC	SHOCK-MC	10 (4.7%)
Combination of CIR and pure HSS fields	CIR-HSS	9 (4.2%)
Combination of shock and CIR fields	SHOCK-CIR	5 (2.3%)
Combination of non-MC ICME and CIR fields	ICME_nc-CIR	2 (0.9%)
Not enough solar wind data to identify the interplanetary structure	Data gap	2 (0.9%)
Combination of ICME MC and CIR fields	MC-CIR	1 (0.5%)
Combination of MC and shock/sheath fields	MC-SHOCK/SHEATH	1 (0.5%)
Combination of pure HSS and CIR fields	HSS-CIR	1 (0.5%)

Table 2

Solar cycle phase	Number of storms	Major IP structures and percentage of storms they caused
Rising phase (1997-1999)	53	CIR/HSS (30.2 %) ICME (24.5 %) SHOCK/ICME (17.0 %) SHOCK/SHEATH (9.4 %)
Maximum (2000-2002)	62	CIR/HSS (33.9 %) ICME (22.6 %) SHOCK/ICME (14.5 %) SHOCK/SHEATH (16.1 %)
Declining (2003-2005)	75	CIR/HSS (60.0 %) ICME (20.0 %) SHOCK/ICME (5.3 %) SHOCK/SHEATH (9.3 %)
Minimum (1996, 2006-2008)	23	CIR/HSS (82.6 %) ICME (8.7 %)

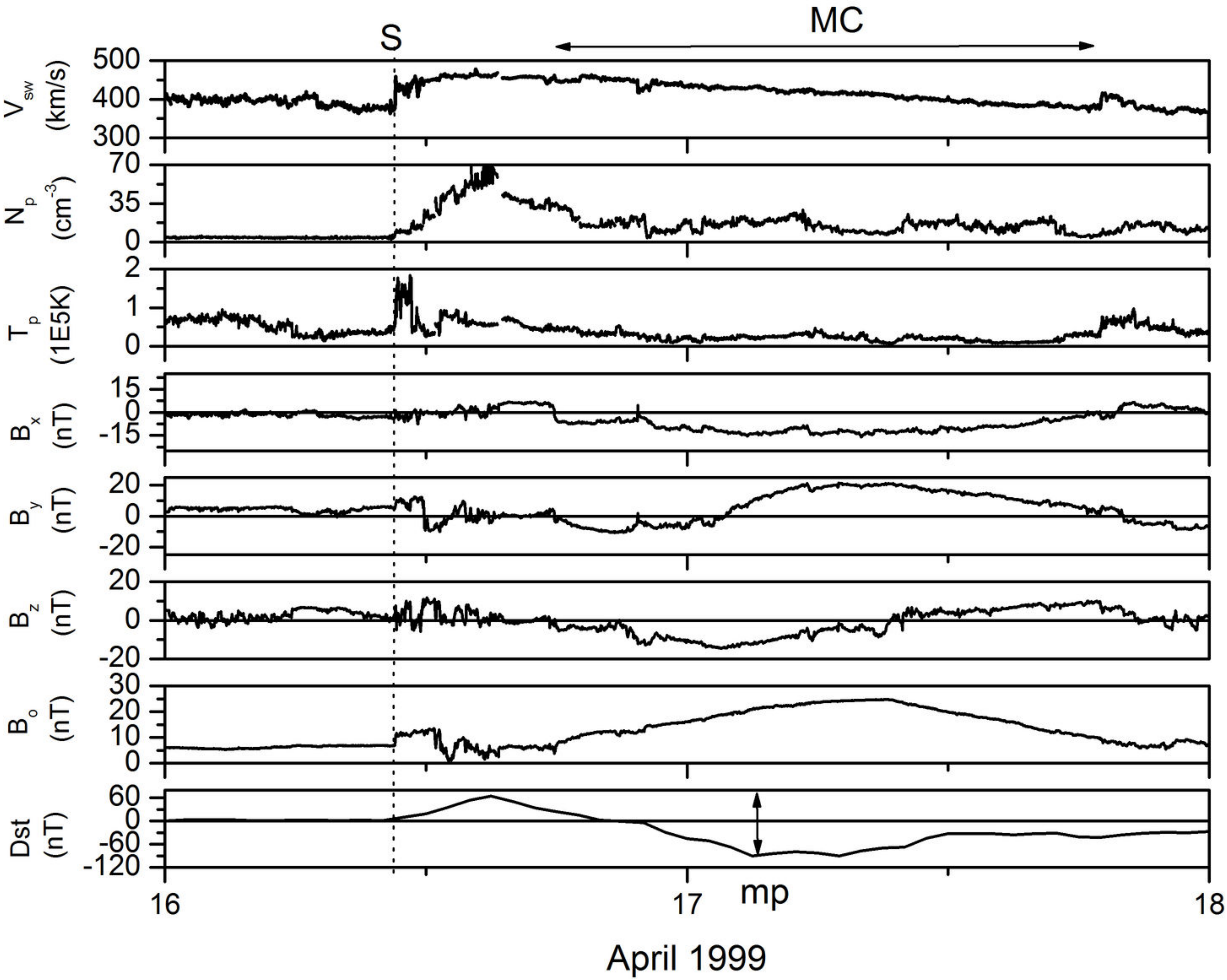

MC
S
V_sw (km/s)
500
400
300
N_p (cm^-3)
70
35
0
T_p (1E5K)
2
1
0
B_x (nT)
15
0
-15
B_y (nT)
20
0
-20
B_z (nT)
20
0
-20
B_o (nT)
30
20
10
0
Dst (nT)
60
0
-60
-120
16
17
mp
18
April 1999

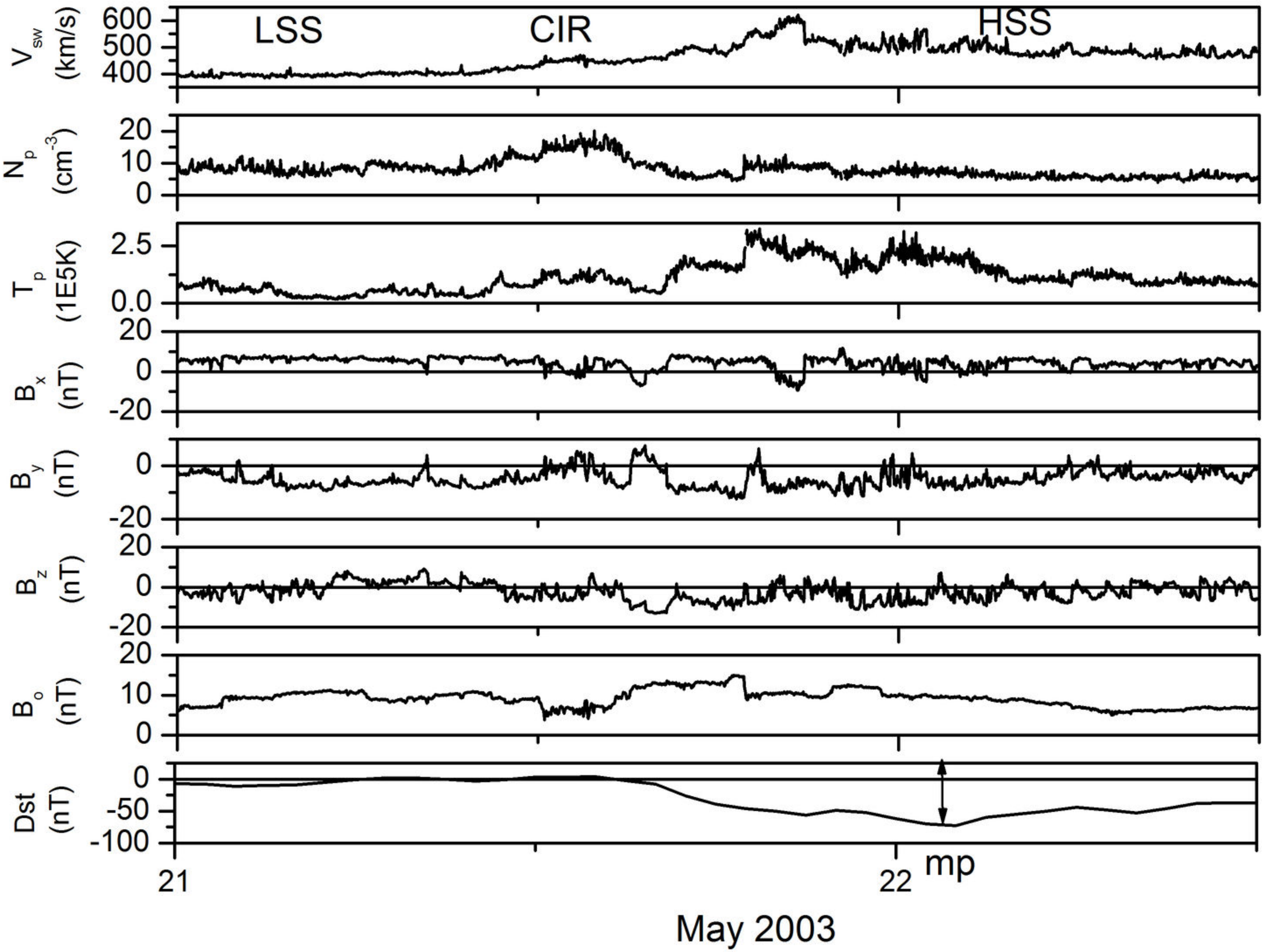

LSS
CIR
HSS
V_{sw} (km/s)
600
500
400
N_p (cm^{-3})
20
10
0
T_p (1E5K)
2.5
0.0
B_x (nT)
20
0
-20
B_y (nT)
0
-20
B_z (nT)
20
0
-20
B_o (nT)
20
10
0
Dst (nT)
0
-50
-100
21
22
mp
May 2003

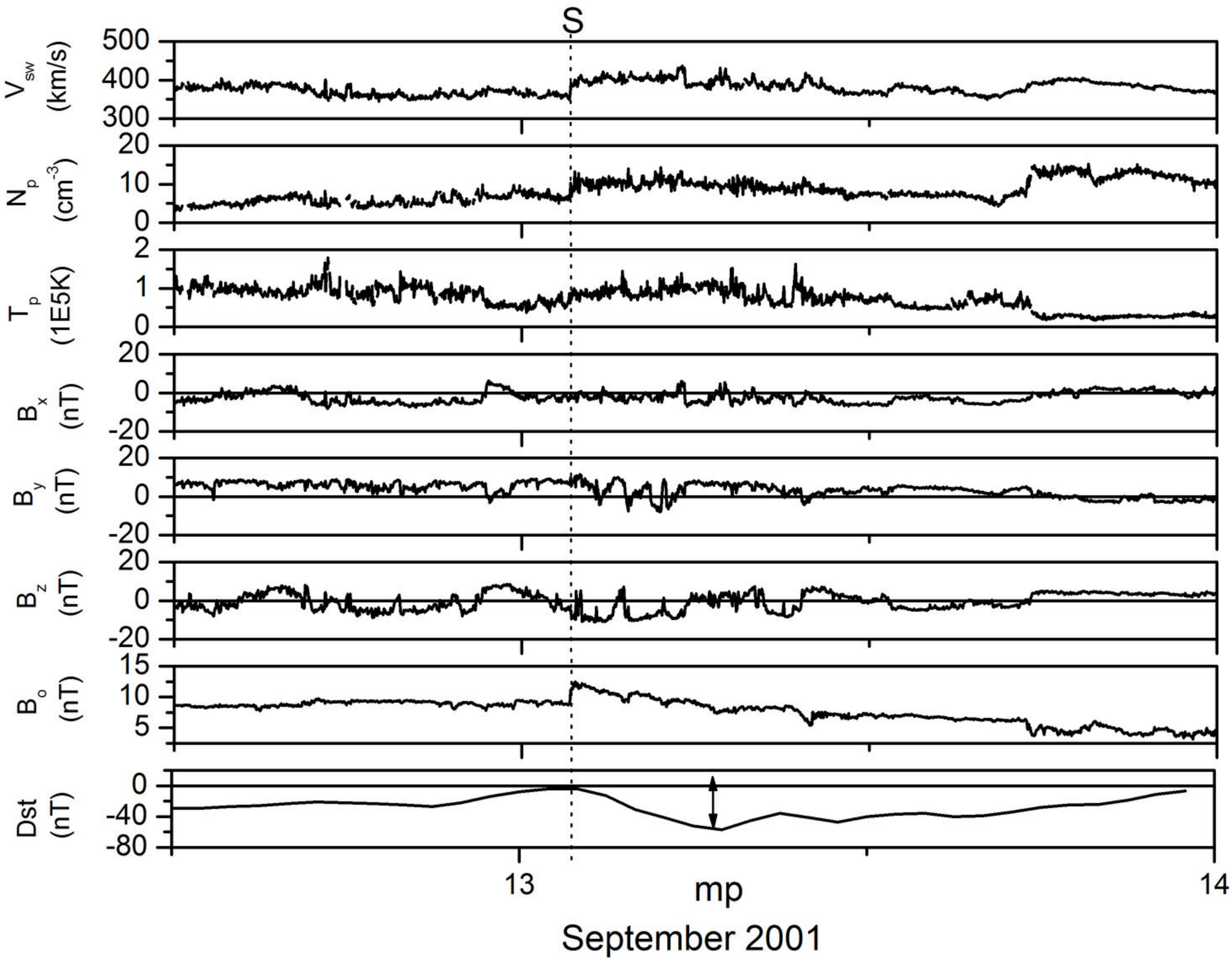
S
V_{sw} (km/s)
500
400
300
N_p (cm^{-3})
20
10
0
T_p (1E5K)
2
1
0
B_x (nT)
20
0
-20
B_y (nT)
20
0
-20
B_z (nT)
20
0
-20
B_o (nT)
15
10
5
Dst (nT)
0
-40
-80
13
mp
14
September 2001

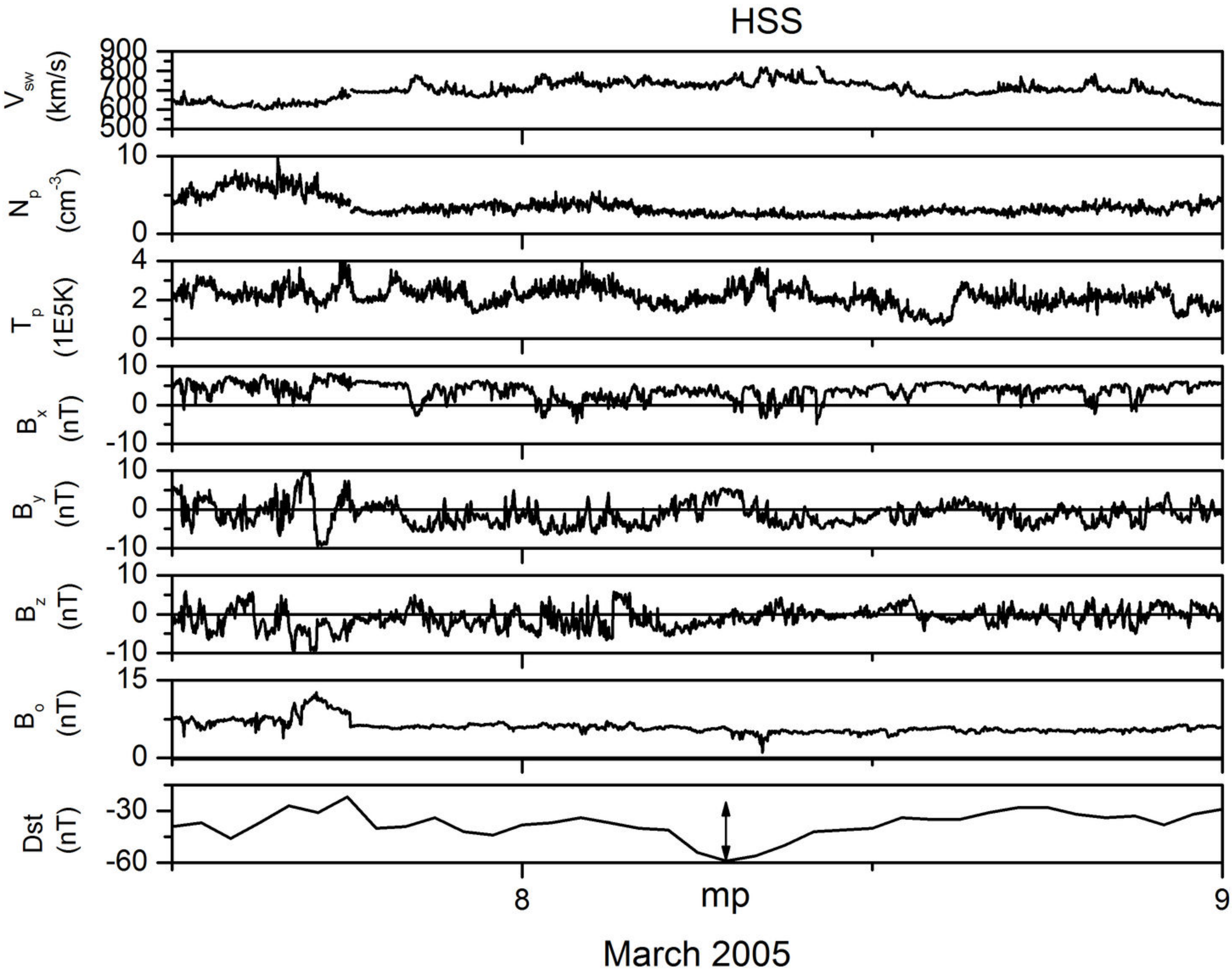

HSS
V_{sw} (km/s)
900
800
700
600
500
N_p (cm^{-3})
10
0
T_p (1E5K)
4
2
0
B_x (nT)
10
0
-10
B_y (nT)
10
0
-10
B_z (nT)
10
0
-10
B_o (nT)
15
0
Dst (nT)
-30
-60
8
mp
9
March 2005

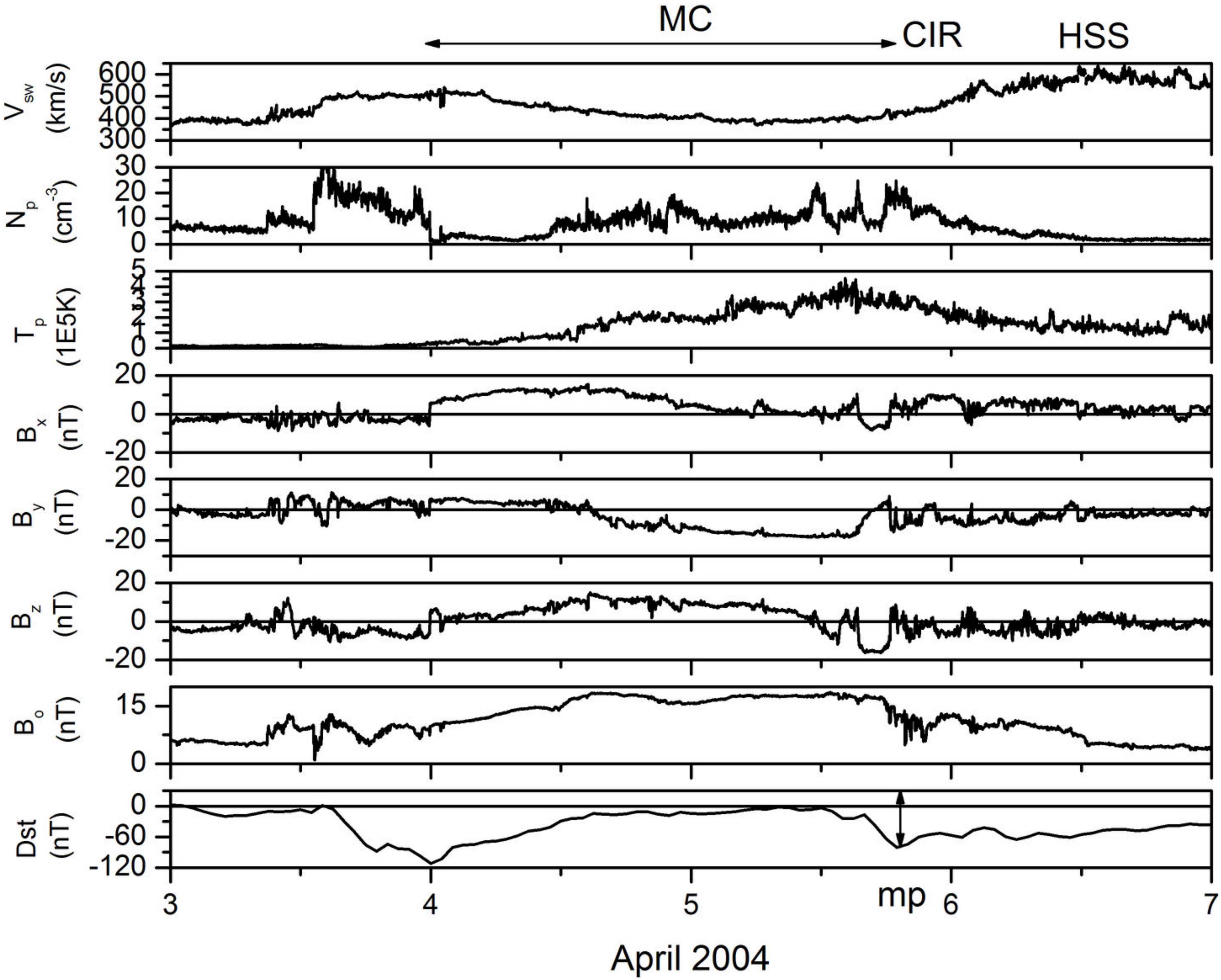
MC
CIR
HSS
V_sw (km/s)
N_p (cm^-3)
T_p (1E5K)
B_x (nT)
B_y (nT)
B_z (nT)
B_o (nT)
Dst (nT)
mp
April 2004

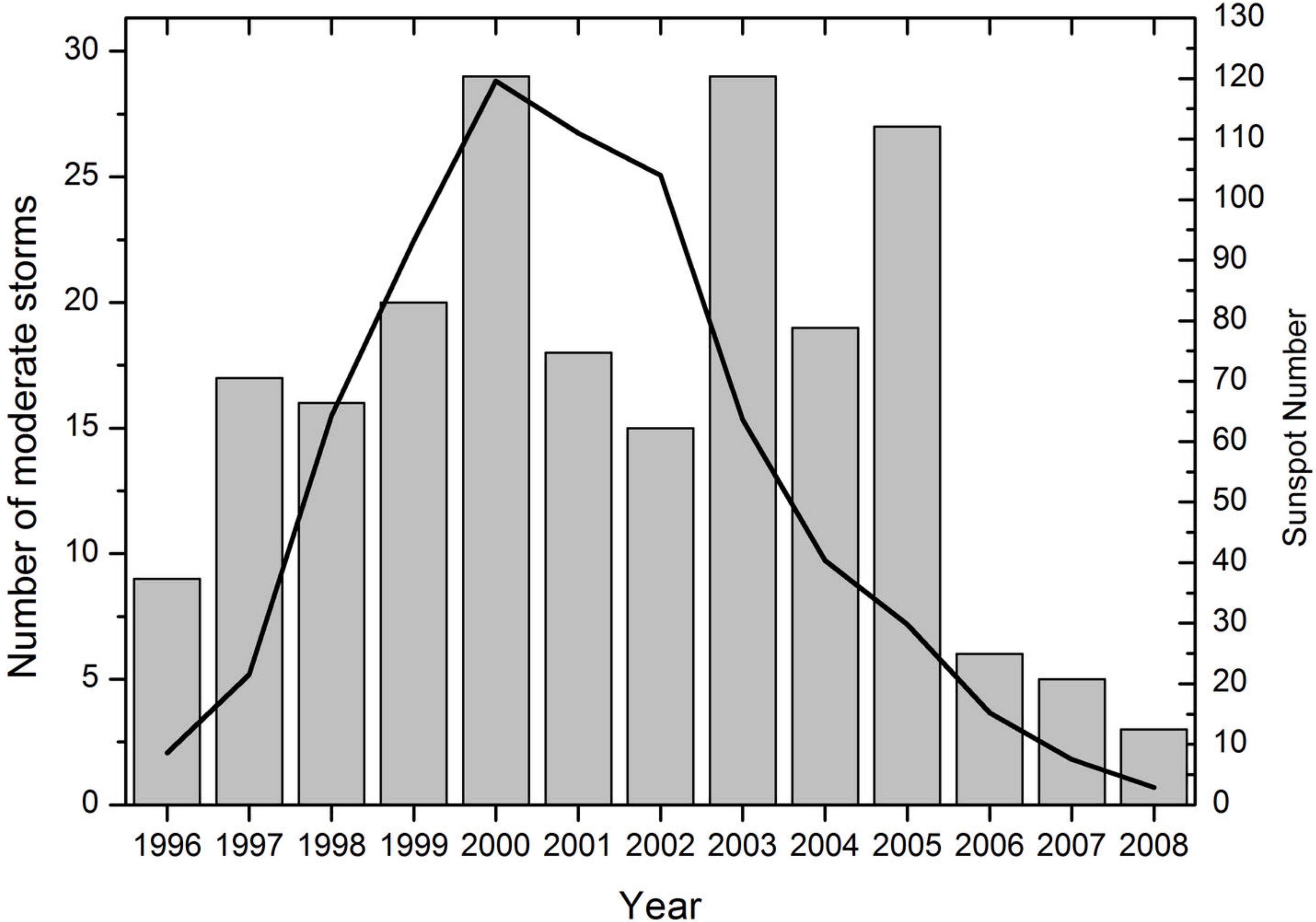

Number of moderate storms
Sunspot Number
Year
0
5
10
15
20
25
30
0
10
20
30
40
50
60
70
80
90
100
110
120
130
1996
1997
1998
1999
2000
2001
2002
2003
2004
2005
2006
2007
2008

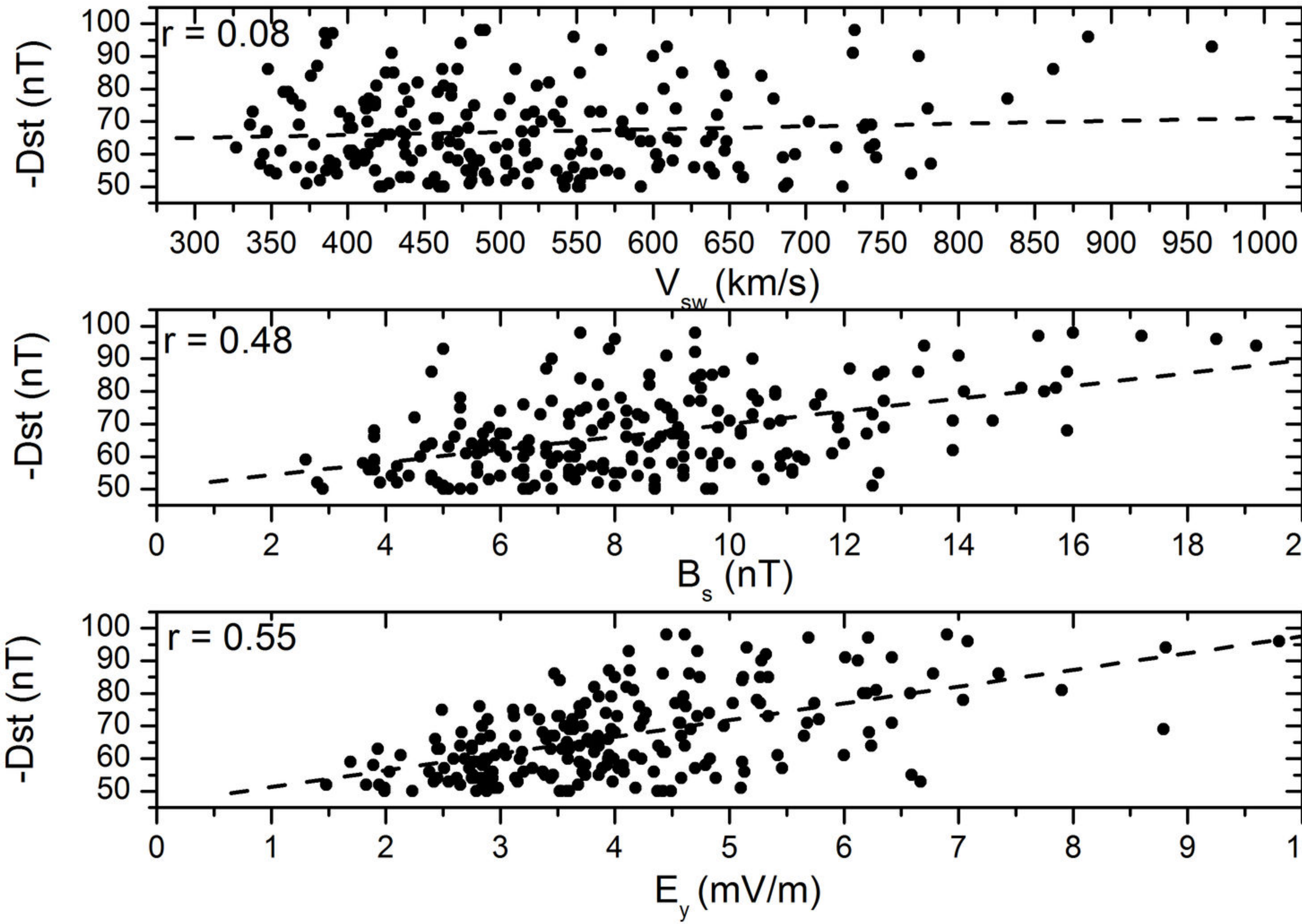
r = 0.08
-Dst (nT)
100
90
80
70
60
50
300
350
400
450
500
550
600
650
700
750
800
850
900
950
1000
V_sw (km/s)
r = 0.48
-Dst (nT)
0
2
4
6
8
10
12
14
16
18
20
B_s (nT)
r = 0.55
-Dst (nT)
0
1
2
3
4
5
6
7
8
9
10
E_y (mV/m)

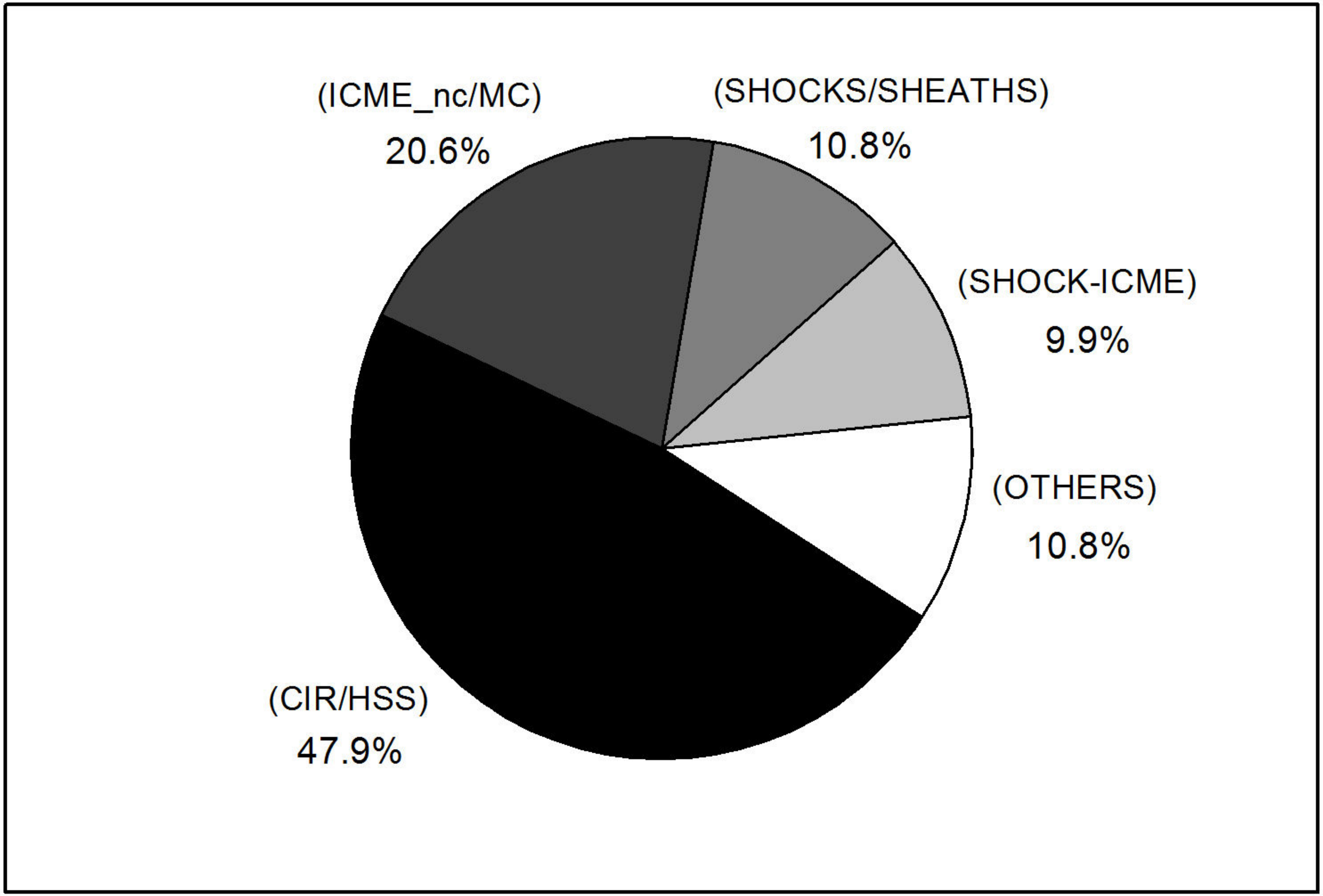
(ICME_nc/MC)
20.6%
(SHOCKS/SHEATHS)
10.8%
(SHOCK-ICME)
9.9%
(OTHERS)
10.8%
(CIR/HSS)
47.9%

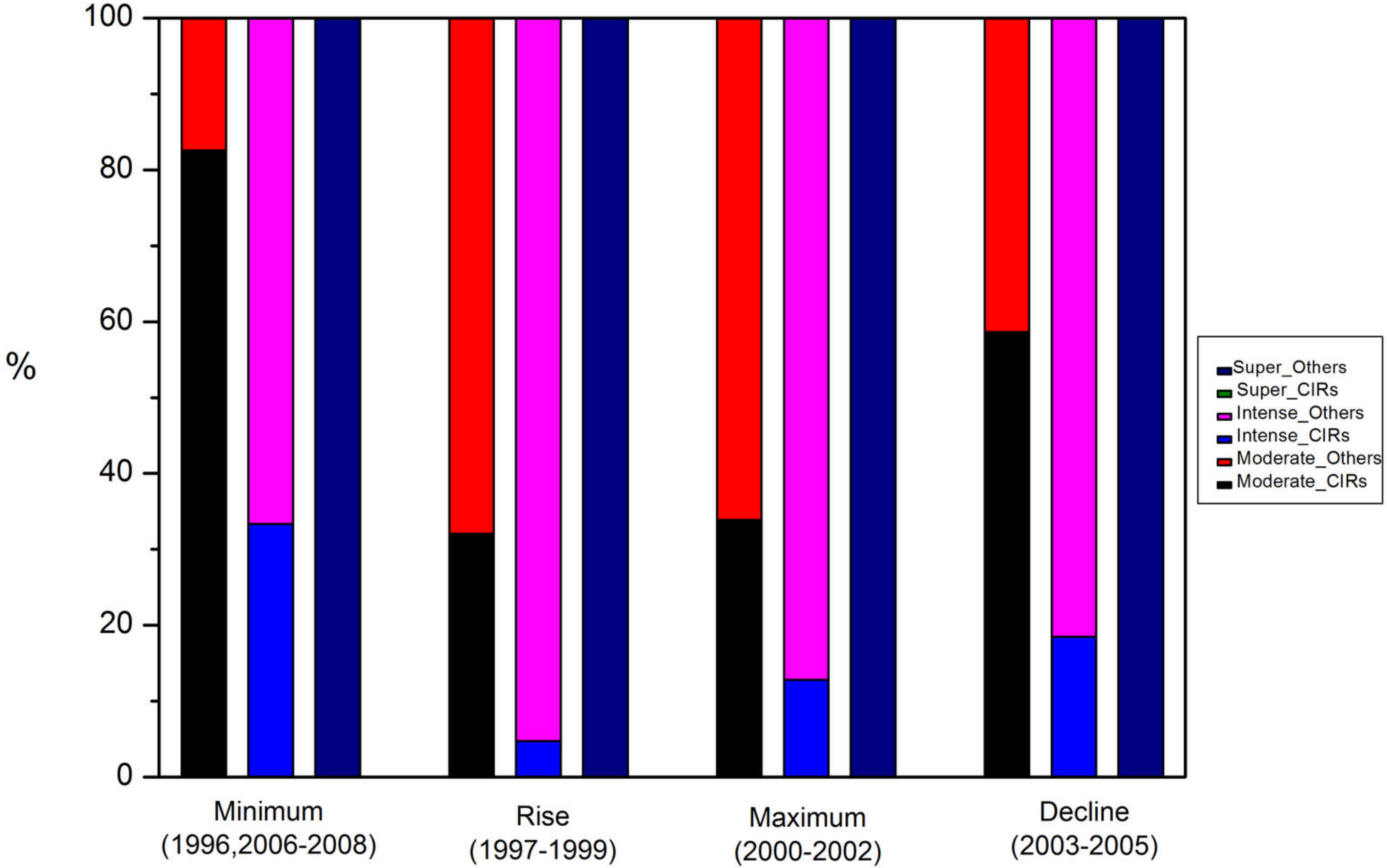
100
80
60
40
20
0
%
Super_Others
Super_CIRs
Intense_Others
Intense_CIRs
Moderate_Others
Moderate_CIRs
Minimum
(1996,2006-2008)
Rise
(1997-1999)
Maximum
(2000-2002)
Decline
(2003-2005)